# Crystallization Behavior of Strongly Interacting Chains

**Amy M. Heintz, Robin L. McKiernan, Samuel P. Gido, Jacques Penelle, and Shaw L. Hsu***

*Polymer Science and Engineering Department and Materials Research Science and Engineering Center, University of Massachusetts at Amherst, Amherst, Massachusetts 01003*

**Sono Sasaki, Atsushi Takahara, and Tisato Kajiyama**

*Department of Applied Chemistry, Kyushu University, Fukuoka, Japan*

*Received October 15, 2001*

ABSTRACT: The crystallization behavior of functionalized polymethylene chains with carbamate esters placed periodically between alternating docosyl and octyl segments has been examined with infrared spectroscopy. Specific features of both the interactions and the chain conformation have been found. The crystallization kinetics, including the induction period, can be followed with time-resolved infrared spectroscopy (5 s time resolution) and occurs in three stages. The kinetics of local hydrogen-bonding rearrangement is quite different from the kinetics of methylene chain stem ordering. The interchain interactions are characterized by a broad distribution of states. The initial melt consists of highly interacting chains (75% hydrogen bonded). During crystallization, this broad asymmetric ensemble of interacting states changes continuously to one dominated by that characteristic of the ordered structure. Even with the time resolution achievable, the specific features of a crystallite nucleus could not be captured.

## Introduction

Polymer crystallization is often best characterized by its kinetics which can be separated into two separate stages: nucleation and growth. While debate still exists regarding precise description of the rate-determining steps,[1,2] this picture of nucleation and growth has been the dominant one and is supported by both morphological and kinetic data on a broad range of polymeric systems.[3,4] More recent data have led some to suggest that under certain conditions order formation may take place through a spinodal decomposition mechanism rather than nucleation.[5−7]

We are interested in beginning to develop a logical framework for clarifying the crystallization behavior of interacting chains. van der Waals interactions alone can describe poly(olefins), but dipole−dipole interactions, hydrogen bonds, and electrostatic interactions are important for many other polymers such as polyesters, polyamides, and proteins. The role of these strong secondary interactions in the crystallization behavior has yet to be defined either experimentally or theoretically. Polyamides serve as excellent examples showing the complexity that seems to arise due to the interplay between hydrogen-bonding interactions, van der Waals interactions, and conformational flexibility. Polyamides can form one of several different polymorphic crystal structures depending on the crystallization conditions or the number of methylene units in the repeat unit.[8] The magnitude and specificity of the amide−amide interaction and the conformational order of the methylene chain segment may have different responses to solvent quality, temperature, cooling and heating rate, or deformation.

Our studies focus on a system of polymers with strongly interacting functionalities placed at exact periodicity along a polymethylene chain as shown in Scheme 1. We are interested in how interchain interactions influence nucleation and growth. The various functionalities contained in these model polymers allow attenuation of the specificity of the interactions, from strong hydrogen bonds to weaker dipole−dipole interactions. In addition, the sequence length of the methylene units can be precisely controlled from 12 to 46 units, allowing variation in the conformational flexibility.

**Scheme 1**

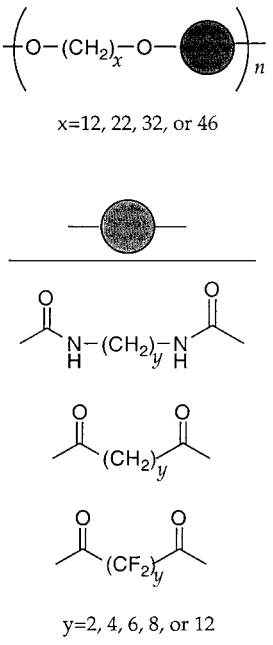


Vibrational spectroscopy has been frequently used to determine the mass fraction degree of crystallinity. Fewer studies have used vibrational spectroscopy to study the crystallization process.[9,10] However, this technique has many advantages that make it ideal for dynamic studies. With the advent of the Fourier transform technique, high-quality spectra can be obtained with time resolution as short as a few seconds. Struc-

* To whom correspondence should be addressed.

10.1021/ma011794k CCC: $22.00 
Published on Web 03/09/2002

tural units can be observed at a localized scale, so long-range coherence is unnecessary. There are other practical considerations. For example, precise temperature control can be achieved easily, and only a small amount of sample is necessary. In addition, a unique feature of vibrational spectroscopy is that the ensemble of chain conformations in the disordered state can be monitored.

A distinction should be made regarding spectroscopically determined "order" vs degree of crystallinity. X-ray diffraction, for example, measures the long-range order as a result of precise atomic placements, while infrared spectroscopy measures short-range order which will depend on the degree to which the vibrational mode is coupled to adjacent vibrations. The short-range order can exist without the presence of long-range order. In this paper, we will refer to a "degree of order" rather than a degree of crystallinity to emphasize the distinction.

In this study, order formation in the strongly interacting units will be observed separately from the straightening of the methylene chains using nonisothermal crystallization conditions, where the most dramatic distinction between the responses of the two parts is observed. Transformations occurring in the disordered phase will be monitored during both the induction period and secondary crystallization. This paper will focus on the system with carbamate esters (urethane units) alternating between 22 and 8 methylene units (22,8 PU).

## Experimental Section

Details of the polymer synthesis and characterization have been reported previously.[11] The polymer was prepared by a melt polyaddition of 1,8-diisocyanatooctane and 1,22-docosanediol. The weight-average molecular weight was determined to be $13.8 \times 10^3$ g mol$^{-1}$, and the polydispersity is 2.0. The melting temperature of the polymer is 141 °C.

Infrared spectroscopic measurements were carried out on a Perkin-Elmer 2000 system with a wide-band MCT detector. Samples were prepared by dissolving the polymer in hot *o*-dichlorobenzene and casting a film onto KBr plates. The plates were dried under vacuum at 90 °C for several hours. No evidence of residual solvent was observed spectroscopically. The resulting films were approximately 15 $\mu$m in thickness.

Measurements of the molten samples were performed with 2 cm$^{-1}$ spectral resolution, and 16 scans were signal averaged. The temperature was controlled using a home-built heating cell attached to an Omega proportional controller that could be accommodated into the $N_2$-purged sample chamber. The temperature was calibrated to the melting point of benzoic acid. Sample temperature was simultaneously monitored using two other thermocouples to ensure thermal equilibrium had been attained in the heating cell. Samples were equilibrated at a given temperature for at least 30 min.

During crystallization experiments, rapid measurements were necessary, so the resolution was set to 4 cm$^{-1}$, and only one scan was needed to obtain high-quality data for analysis. A Mettler hot stage was used to control the temperature and cooling rate to within an accuracy of ±0.6 °C. The sample was sandwiched between two KBr plates and placed in the hot stage. This hot stage was then mounted in the $N_2$-purged sample chamber, and sufficient throughput could be obtained. Spectra were recorded approximately every 5 s. The melted sample was held at 160 °C (20 °C over the melting point) for at least 30 min. The length of time held in the molten phase was used to prevent any possibility that memory remains.[8] During this holding time, the infrared spectrum was monitored, and no spectral changes were seen after the first minute. We also observed higher holding temperatures (up to 185 °C) and found that 160 °C was sufficient to remove any spectroscopic evidence of crystallinity. The molten phase was then crystallized at a given cooling rate ranging from 2.5 to 15 °C min$^{-1}$.

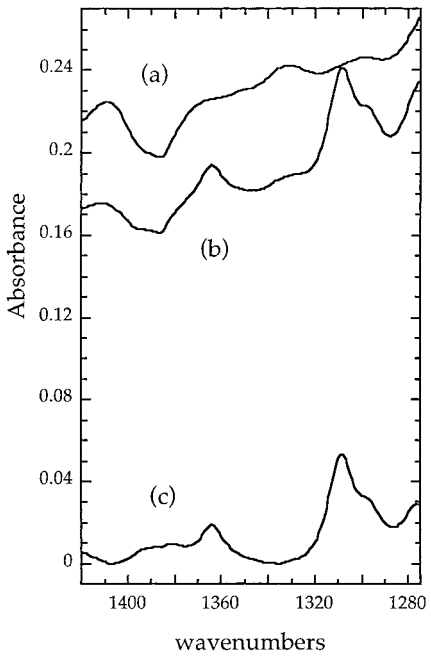


**Figure 1.** Procedure used to observe the ordering of aliphatic segments from the infrared spectra of 22,8 PU. The spectrum observed from the disordered phase (a) was subtracted from spectra collected during crystallization (b) to give a spectra indicative of ordered methylene segments (c).

Band deconvolution of the amide I region was carried out following the procedure established previously.[12] It has been demonstrated that this region is appropriately characterized by three components: (1) free C═O at 1732 cm$^{-1}$, (2) hydrogen-bonded C═O with an ordered geometry (such as the one the crystalline state) at 1685 cm$^{-1}$, and (3) hydrogen-bonded C═O with disordered geometries between 1718 and 1709 cm$^{-1}$. This band is associated with a distribution of distances and geometries of hydrogen bonds. Three Gaussian bands were employed for deconvolution. The program included in the Spectrum 2000 software package associated with our Perkin-Elmer system 2000 spectrometer was used for all analysis. The band position, width, and intensity were allowed to change during iteration. The ensemble of hydrogen bonds of varying strength was obtained by removing the contributions from the free and ordered vibrations.

To observe crystallization of the methylene chains, the contribution from disordered sequences was subtracted, as shown in Figure 1. The intensity at 1405 and 1335 cm$^{-1}$ arises from particular methylene defect sequences in the molten or amorphous phases.[13] The spectrum of the disordered structure was defined in the region from 1270 to 1420 cm$^{-1}$ by the spectrum obtained immediately prior to crystallization. Different percentages of this spectrum were subtracted from the succeeding spectra so that the baseline at 1405 and 1335 cm$^{-1}$ was zero. The remaining contribution is from the "straight" methylene sequences. The intensity increases as the low wavenumber side is approached due to the contribution from the amide III mode near 1250 cm$^{-1}$.

The rate of primary crystallization for various cooling rates was determined from the increase in intensity of the ordered hydrogen bonds (1684 cm$^{-1}$) with time using numerical differentiation

$$\left.\frac{dI_{1684}}{dt}\right|_j = \frac{I_j - I_{j-1}}{t_j - t_{j-1}} \quad (1)$$

We found the spectroscopic data obtained to be of high quality with good signal-to-noise ratio for this analysis to be carried out readily.

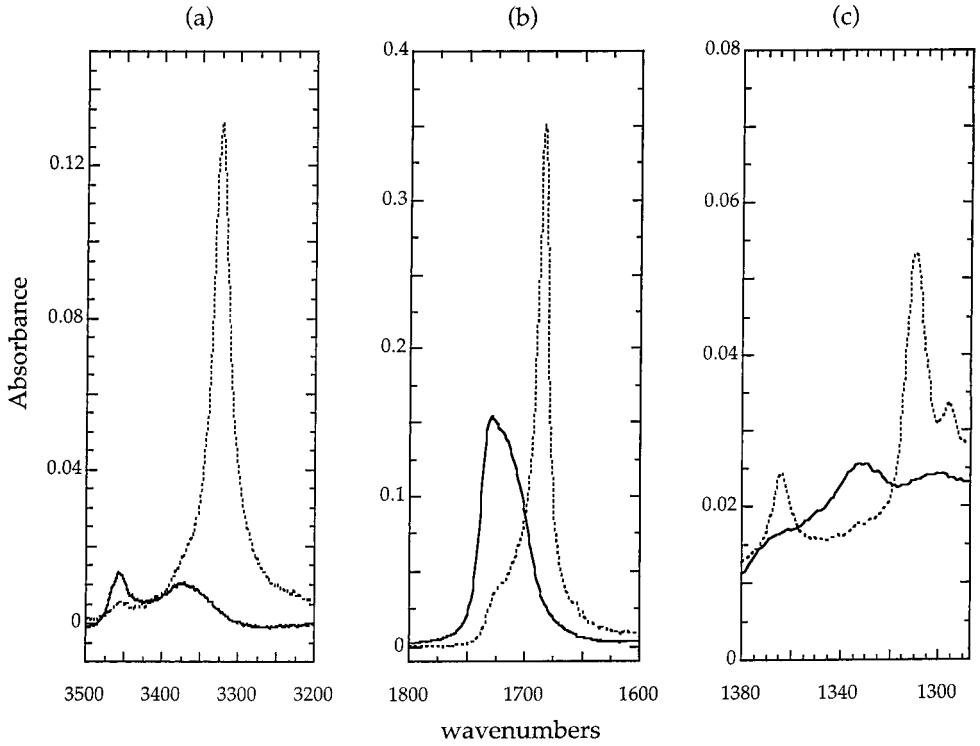


**Figure 2.** Infrared spectra of molten 22,8 PU (160 °C; solid lines) and a melt crystallized film (25 °C; dashed lines): (a) the N−H stretching region; (b) the amide I, C═O stretching region; (c) methylene wagging modes.

## Results and Discussion

**Infrared Spectroscopic Features Characteristic of 22,8 PU.** To take advantage of the sensitivity of infrared spectroscopy to local geometry, interchain interactions, and chain conformation, the origin of the vibrational features associated with 22,8 PU must first be defined. First, the urethane interchain interactions, i.e., hydrogen bonds, will be considered. Hydrogen bonds are dynamic, continually breaking and re-forming under the influence of thermal fluctuations. The urethane groups thus consist of a distribution of species, both free (non-hydrogen-bonded) and hydrogen-bonded. Historically, the existence of hydrogen bonds has been most readily illustrated from changes in the N−H stretching region, shown in Figure 2a for 22,8 PU. The inherent resonance contribution to the relative intensities of the 3456 (free NH), 3370 (hydrogen-bonded in melt), and 3322 $cm^{-1}$ (ordered hydrogen bond) bands make using this region for quantitative analysis more difficult.[14] The measured absorption coefficient of the hydrogen-bonded component is strongly dependent on the strength of hydrogen bond.[15] Therefore, the apparent measured relative intensity of the hydrogen-bonded and the free component are not indicative of the relative population of each species. Using these bands can, in fact, lead to misleading conclusions regarding the estimation of the enthalpy of hydrogen bond formation.[14]

On the other hand, the frequency difference, $\Delta\nu$, between free and hydrogen-bonded species can be related to the strength of the hydrogen bond. The enthalpic contribution can be determined using the following expression[16]

$$-\Delta H_{\text{sp.int}}^{\text{NH/O=C}} = \frac{59.3\Delta\nu}{\Delta\nu + 674} \qquad (2)$$

Using this approach, we can determine the strength of the hydrogen bond in the initial state (the melt). A large interchain interaction in the range from −7.03 to −6.40 kJ $mol^{-1}$, depending on the temperature, was obtained.

The amide I band (mainly C═O stretching) reflects the strength and geometry of hydrogen-bonding as well as the number of interacting species in 22,8 PU (see Figure 2b). This region is more appropriate for quantitative analysis due to the relative insensitivity of the absorption coefficient to hydrogen bond strength. Because the bands owing their intensity to free C═O (1732 $cm^{-1}$), disordered hydrogen-bonded C═O (1718−1709 $cm^{-1}$), and ordered hydrogen bonds (1685 $cm^{-1}$) are overlapping, we employ a curve-fitting routine to resolve the amount of each species, as shown, for example, in Figure 3a. Results for molten samples are shown in Table 1. The absorption coefficients for the free species are slightly lower than that for the associated species but were corrected for by adjusting the hydrogen-bonded intensities by a factor, $k = 1.81$, so that the total area remained invariant with temperature. This then allows us to calculate the fraction of each species present.[12]

Using these separated fractions, we can determine the thermodynamic properties of the molten phase. By assuming that the urethane units associate as hydrogen-bonded dimers, the equilibrium constant can be determined from the fraction of free urethanes by[17]

$$K_{\text{eq}} = \frac{1 - [\text{C=O}]}{2([\text{C=O}])^2} \qquad (3)$$

As shown in Figure 3b, the enthalpy and entropy of hydrogen bond formation can be determined from a van't Hoff plot. The $\Delta H$ of hydrogen bond formation ($\Delta H_{\text{HB}}$) was determined from this procedure to be −7.20 kJ $mol^{-1}$. The $\Delta S_{\text{HB}}$ was found to be −2.09 J $mol^{-1}$ $K^{-1}$.

Thus, both methods have yielded similar interaction values for the initial, molten phase. The enthalpic

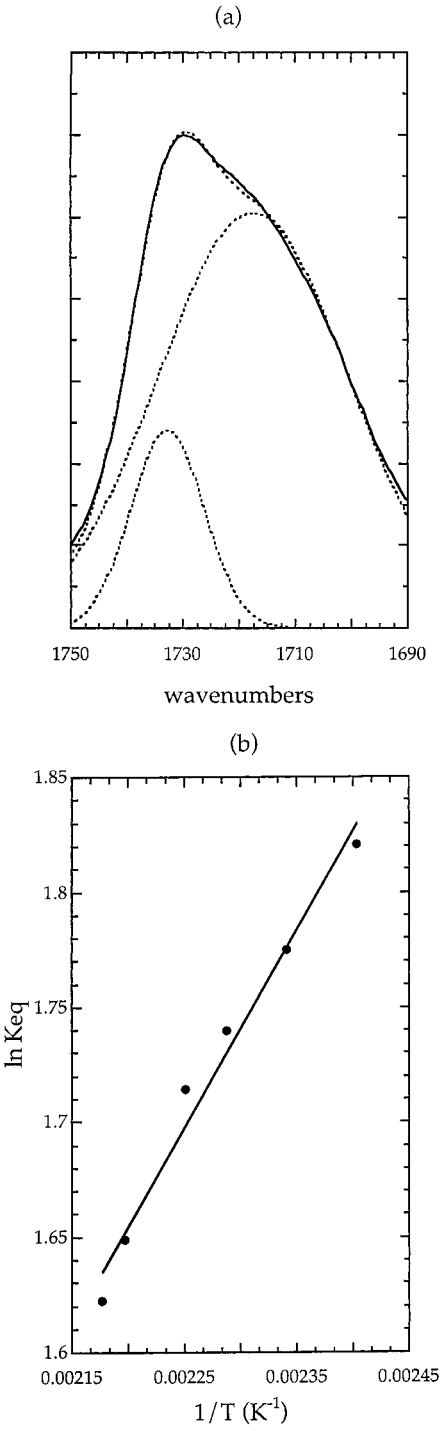


**Figure 3.** Characterization of the molten phase of 22,8 PU: (a) infrared spectrum in the amide I region (solid line) and the free and disordered hydrogen-bonded components obtained using band deconvolution routine described in the Experimental Section (dashed lines); (b) a van't Hoff plot based on the concentration of free carbonyls found (Table 1).

difference, $\Delta H_{HB}$, is approximately −7.11 kJ mol$^{-1}$ per urethane or −14.22 kJ mol$^{-1}$ per repeat. Spectroscopic data show that approximately 75% of the urethane groups are hydrogen-bonded in the melt at any particular time. Given the motions available to the polymers, this picture is a dynamic one averaging many possible states. Nonetheless, the strong specific interactions will play the role of effective cross-links. It has been shown that hydrogen bonds hinder relaxation.[18] As we shall demonstrate, this factor affects both the nucleation and growth of strongly interacting polymers.

The strength and geometry of urethane hydrogen bonds characterize the interchain interactions. A description of the single chain properties is evaluated by the conformational order of the aliphatic segments. Among all the characteristic vibrations of the methylene sequence, the methylene wagging vibration is most easily analyzed for the crystalline state. These modes have been used to characterize the crystallinity of other aliphatic polyurethanes.[19] The region from 1280 to 1380 cm$^{-1}$ is shown in Figure 2c.

In the melt, only the broad component at 1335 cm$^{-1}$ associated with disordered chains is found. Upon crystallization, several new bands appear as part of the methylene wagging progression series for the octyl and docosyl segments. The methylene units in a particular segment can be modeled as a series of coupled oscillators. Usually the nearest neighbors are considered. As a result, the vibration of each methylene unit becomes nondegenerate. In this case, instead of observing one wagging vibration, a progression of several vibrations is observed. For a chain of parallel dipoles the frequency is related to the segmental length by

$$\omega^2 = \omega_0^2 + 4\omega'^2 \sin^2 \frac{d\mathbf{k}}{2} \qquad (4)$$

where $\omega'$ is related to the intramolecular coupling force constant, $d$ is the distance between two oscillators, and $\mathbf{k}$ is the wave vector. The observed frequencies are sensitive to both the numbers of units in a segment and the conformation. Changes in these bands are characteristic of conformational changes of an entire segment. The bands at 1308 and 1361 cm$^{-1}$ can be attributed to the octyl segments while the band at 1296 cm$^{-1}$ owes its intensity to the docosyl segment.[20]

**Spectroscopic Changes upon Melting 22,8 PU.** To validate our choice of the 1685 and 1308 cm$^{-1}$ regions as appropriate monitors of the urethane and methylene segments, we observed the changes in the infrared spectra of 22,8 PU upon melting at a heating rate of 10 °C min$^{-1}$, as shown in Figure 4. Immediately upon heating, a linear decrease in the intensity at1308 cm$^{-1}$ is observed. The hydrogen bonds, on the other hand, are stable. Around 90 °C, the decrease in aliphatic order accelerates, and on the basis of data from polyamides, this behavior may coincide with a Brill transition.[8] Changes in the hydrogen-bonded state are not observed until a temperature near 120 °C is reached. Finally, the structure melts at 135 °C. These results are consistent with the changes seen upon melting of nylon-6,6.[21] Solid-state NMR studies of nylon-6,6 showed that, upon heating, the individual methylene groups exhibit librational motion within the crystal, whereas the hydrogen-bonded amides remain relatively immobile. As temperatures near the melting point are approached, the amplitude of the methylene librations becomes very large, and the number of ordered hydrogen bonds decreases. Similarly, for the case of 22,8 PU, a structural disordering is initiated first in the methylene chain stem as observed from the intensity redistribution at 1308 cm$^{-1}$. The main point here is that the two vibrations chosen to describe the model polymer, 1685 and 1308 cm$^{-1}$, correlate with specific structural changes in the crystal.

**Kinetics of Thermal Crystallization.** Having validated that these infrared vibrations correspond to

**Table 1. Results from Curve Fitting of Amide I Region**

| | disordered H bonds | | | free carbonyls | | | | | |
|---|---|---|---|---|---|---|---|---|---|
| temp (°C) | position ($cm^{-1}$) | width ($cm^{-1}$) | area | position ($cm^{-1}$) | width ($cm^{-1}$) | area | total | total[a] | [free] |
| 143 | 1716 | 39.8 | 20.75 | 1732 | 15.2 | 3.72 | 24.47 | 15.06 | 0.247 |
| 154 | 1717 | 39.8 | 20.53 | 1732 | 15.2 | 3.78 | 24.31 | 14.99 | 0.252 |
| 164 | 1717 | 39.8 | 20.49 | 1732 | 15.3 | 3.84 | 24.33 | 15.04 | 0.256 |
| 171 | 1718 | 39.8 | 20.45 | 1732 | 15.3 | 3.89 | 24.34 | 15.07 | 0.258 |
| 182 | 1718 | 39.8 | 20.22 | 1732 | 15.5 | 4.00 | 24.22 | 15.05 | 0.266 |
| 186 | 1719 | 39.8 | 20.11 | 1733 | 15.6 | 4.04 | 24.14 | 15.02 | 0.269 |

[a] Total area corrected by a factor ($k$) as described in the text.

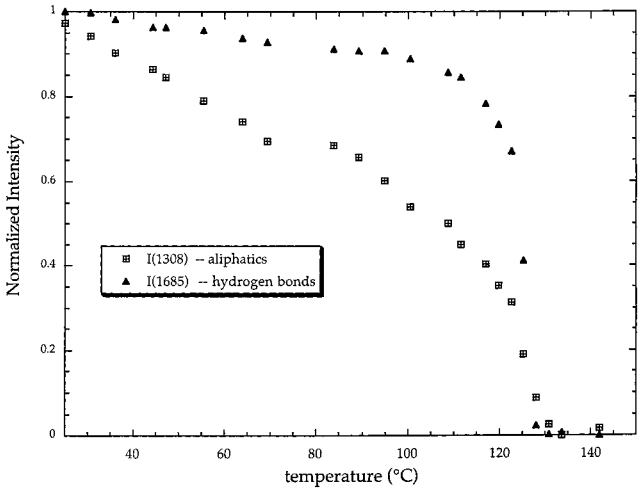


**Figure 4.** Changes in the band intensity associated with ordered hydrogen-bonded urethane units (1685 $cm^{-1}$) and methylene segments (1308 $cm^{-1}$) upon melting 22,8 PU. The heating rate is 10 °C $min^{-1}$. Intensities have been normalized to the initial state.

specific structural changes, we wanted to observe the correlation between interchain interactions and segmental ordering during crystal formation. 22,8 PU was crystallized at several different cooling rates ranging from 2.5 to 15 °C $min^{-1}$, and the infrared spectra were simultaneously collected. Isothermal conditions are conventionally used to study polymer crystallization. We also tried isothermal conditions for this system, but we found that thermal conditions are most effective for observing differences in the kinetics of order formation between the two parts. Nonisothermal crystallization conditions will give a broader distribution of crystal thicknesses. These conditions will also produce a sharper onset of crystallization. This last aspect can be varied by changing the cooling rate.

The changes that occur in the amide I region upon crystallization of 22,8 PU with a cooling rate of −5 °C $min^{-1}$ are shown in Figure 5a. At the onset of crystallization, a sharp increase is seen in the ordered hydrogen-bonded (1684 $cm^{-1}$) component. This is accompanied by a simultaneous decrease in the number of free urethanes and disordered hydrogen bonds. After this initial stage, defined to be primary crystallization, the crystallization rate diminishes significantly as shown. Order formation then continues to consume both free and disordered hydrogen bonds. Disordered hydrogen bonds can exist either within the amorphous phase or within the crystal. The free urethanes, on the other hand, can only exist in the amorphous phase or at the lamellar surface. In fact, it has been suggested that the ratio of ordered hydrogen bonds to free urethanes should be related to this crystal thickness.[14] The second crystallization stage could then be made up of two different

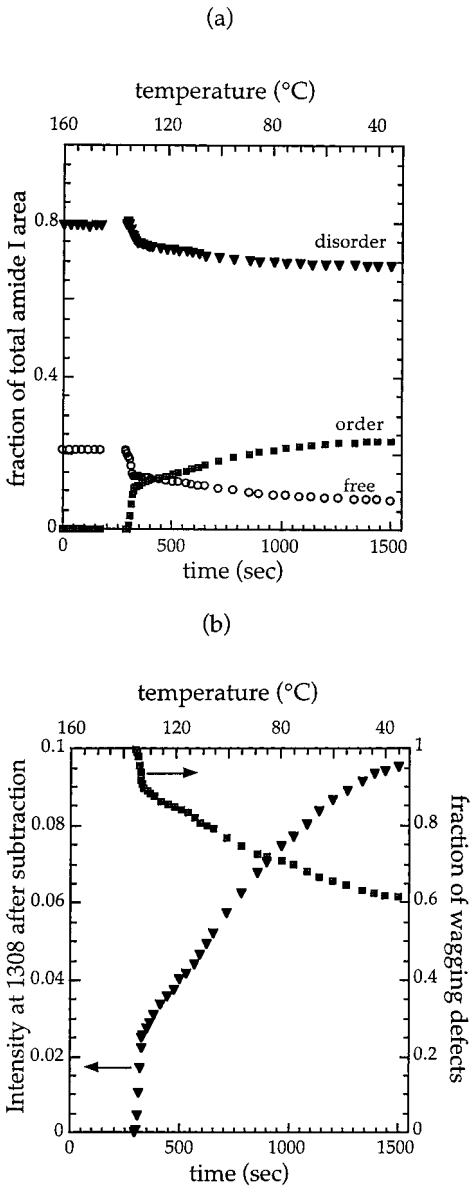


**Figure 5.** Crystallization behavior of 22,8 PU when cooled at a cooling rate 5 °C $min^{-1}$: (a) changes in the urethane units based on the relative intensities of the various components found in the amide 1 (C═O stretching) region; (b) changes in the aliphatic conformation based on the methylene wagging band in the1308 $cm^{-1}$ region (see text).

processes: conversion of amorphous material to crystal or the removal of defects within the crystal. From the relative intensities measured, the total amount of hydrogen-bonded component reaches 90%. If we take the sharp 1684 $cm^{-1}$ band to represent the volume fraction of fully crystalline structure, we obtain a degree of order of 25% at 1500 s. This value is comparable to

the degree of crystallinity generally associated with neat aliphatic nylons.[8]

Our analysis suggests that an additional component might exist at 1692 $cm^{-1}$. However, the contribution of this component contributes at most 5% to the overall intensity in this region. Two crystalline phases were detected in X-ray diffraction experiments: one triclinic showing strong intensities at 3.7 and 4.6 Å and the other pseudohexagonal showing a diffuse intensity at 4.1 Å.[22] The contribution from the pseudohexagonal phase is most apparent in rapidly quenched samples.

Simultaneously, we also observed order formation of the methylene segments as shown in Figure 5b. After removing the amorphous contribution of the disordered band at 1335 $cm^{-1}$, it is possible to monitor the sharp prominent 1308 $cm^{-1}$ $CH_2$ wagging band in this region. The intensity of this component and the amount of the amorphous contribution is plotted in Figure 5b. As was seen for the urethane components, the spectroscopic features of the aliphatic segments also exhibit different rates of change associated with different stages of crystallization. During the second stage, defined to be secondary crystallization, the position of the $CH_2$ wagging progression band typically shifted 4 $cm^{-1}$ higher from 1306 to 1310 $cm^{-1}$. This result was typical for crystallization at several cooling rates (2.5−15 °C $min^{-1}$) and was not correlated to temperature. Rather, this shift must be related to segmental conformation changes that occur during secondary crystallization. A measure of the conformational order associated with the polymethylene chains can be deduced from the intensity of the wagging defect band. Our analysis indicates that 40% of the polymethylene sequences exhibit conformational order.

We were intrigued by the difference in the order achieved associated with interchain interactions represented by hydrogen bonds (25%) vs the conformational order represented by the number of ordered chain stems (40%). In polymers, polymorphism suggests that conformational order does not necessarily correlate to packing order. For example, the interchain interactions in polyethylene are completely disrupted during the phase transition from the orthorhombic to the hexagonal state, yet the chain stem maintains its straightness.[23]

For 22,8 PU, the kinetics is also quite different for the two aspects of structural transformation. The kinetics of conformational order in comparison to interchain order formation is shown in Figure 6. To relate the differences between the hydrogen bonds and the aliphatic conformation, the intensities observed at 1685 and 1308 $cm^{-1}$ were normalized to the final state. Crystallization was marked by three stages. In the initial stage, both hydrogen bonds and chain conformation form order quickly and at a similar rate. Relatively speaking, the hydrogen bonds form a higher degree of order than the methylene segments in this initial stage, but as shown in Figure 5, the degree of order at this point is ∼12% based on both hydrogen bonding and aliphatic conformation. This first stage of crystallization is followed by a slower, but linear, increase in the urethane and aliphatic order. In this second stage, conformational order forms slightly faster and to a higher degree compared to the order achieved by the hydrogen bonds. The third stage is characterized by the point where the kinetics of interchain and conformational order formation deviate from each other, for example, at the 750 s interval when the cooling rate is 5 °C $min^{-1}$. At this time, the rate of order formation

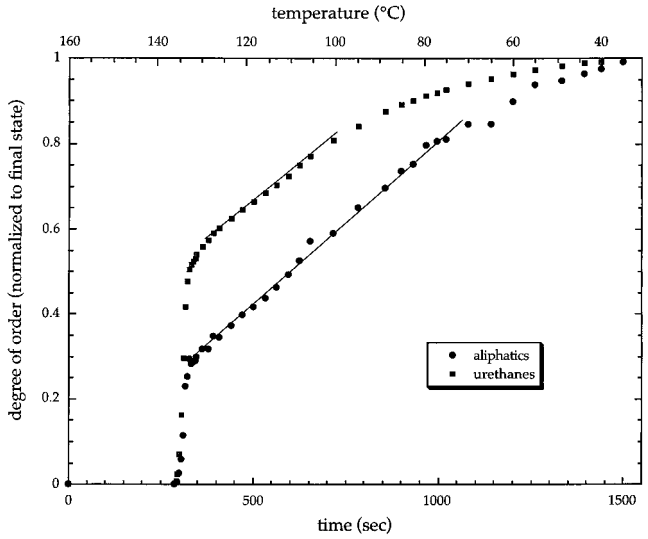


**Figure 6.** Kinetics of ordered hydrogen bond formation (intensity at 1685 $cm^{-1}$) vs aliphatic conformational order (intensity at 1308 $cm^{-1}$) during melt crystallization. The cooling rate is maintained at 5 °C $min^{-1}$. Intensities are normalized to the final state.

begins to diminish for the urethanes. The aliphatic segments, on the other hand, dominate the crystallization process here for another 250 s. This behavior was observed for all crystallization rates ranging from 2.5 to 15 °C $min^{-1}$. However, the transition point to this third stage is independent of temperature.

Various stages of structural ordering have been seen in other polymers. Combined spectroscopic and light scattering studies on the crystallization of syndiotactic polystyrene have suggested that conformational changes during the onset of order formation are related to the orientation fluctuations that ultimately lead to crystallization.[24] Density fluctuations (5−40 nm) have been observed by small-angle X-ray scattering (SAXS) prior to reflections in wide-angle X-ray diffraction (WAXD) during melt crystallization of polyethylene, isotactic polypropylene, and poly(butylene terephthalate) and cold crystallization of quenched aromatic polyesters, which suggests that the order formation process may not be an instantaneous one.[25−27]

**Transformations in the Disordered Phase.** The different crystallization regimes observed for 22,8 PU can be monitored in more detail by observing changes in the disordered interchain interactions. Figure 7 shows the amide I disordered band shapes (free and ordered components have been subtracted) at several representative points along the crystallization curve. This asymmetric band shape reflects the population of hydrogen bond strengths and changes in the population as the crystallization occurs. At the start of crystallization ($t = 0$), the system is at equilibrium in the melt. The broad band shape is somewhat asymmetric with a full width at half-maximum (fwhm) of 34 $cm^{-1}$ and considerable intensity at 1716 $cm^{-1}$. Prior to crystallization (for example at $t = 284$ s), both a change in the position and an increase in fwhm are observed. This behavior was also observable from the raw data. In each of the crystallization experiments performed, a continuous increase in the fwhm of the amide 1 band was always observed. No features of crystalline structure are evident at this time. The changing shape of this band represents a continuous transformation of disordered states into more favorable ones. The order formation or

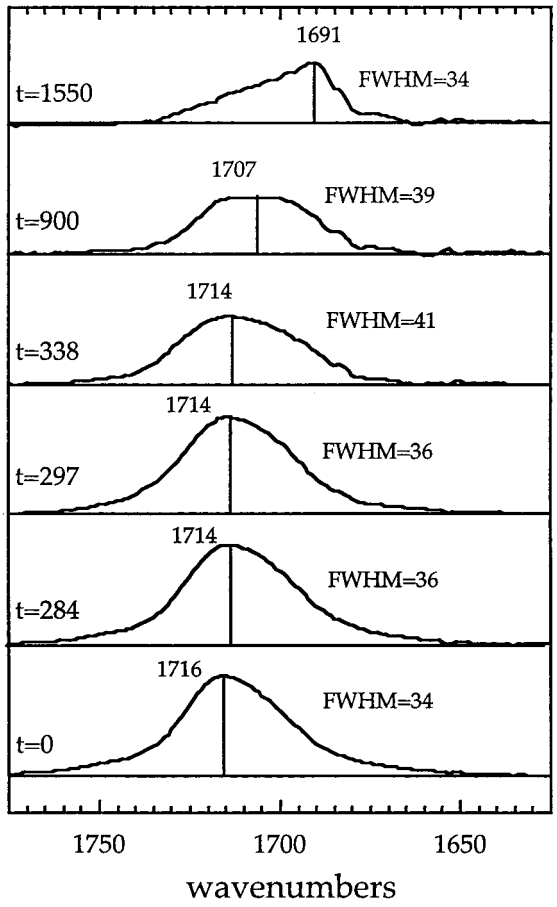


**Figure 7.** Changes in the amide I disordered band during crystallization at a cooling rate of 5 °C min$^{-1}$. The C=O stretching bands associated with free and ordered hydrogen-bonded urethane units have been subtracted.

crystallization of these model polyurethanes clearly is not a discontinuous process. We find the induction period encompasses an entire distribution of interactions of different strength. The entire ensemble evolves into a more ordered state over a time scale slower than we expected.

As shown in Figure 7 the secondary crystallization is also characterized by the presence of a broad distribution of hydrogen bond strengths. This ensemble is reflected in the intensity and particularly the shape of the composite band in the region of 1691 cm$^{-1}$ between the well-defined free component and the ordered one. At the start of secondary crystallization ($t$ = 338 s), the maximum position remains fixed, although an increase in fwhm is observed. The most dominant population shifts to lower wavenumber, which is associated with refinement in geometry. The changing shape of the disordered composite band reflects either crystallization of the amorphous phase or crystalline perfection. Growth in these domains is evidently inhibited. After crystallization is complete, the disordered band is highly asymmetric with a maximum intensity at 1691 cm$^{-1}$. The amorphous regions are not liquidlike. This band observed in the final stage does not resemble the band observed in the initial liquid phase.

**Determination of the Energy Changes during Crystallization.** The crystallization rates for the initial crystal formation as a function of different cooling rates are shown in Figure 8a. As expected, we observed higher rates of crystallization and at larger supercooling for

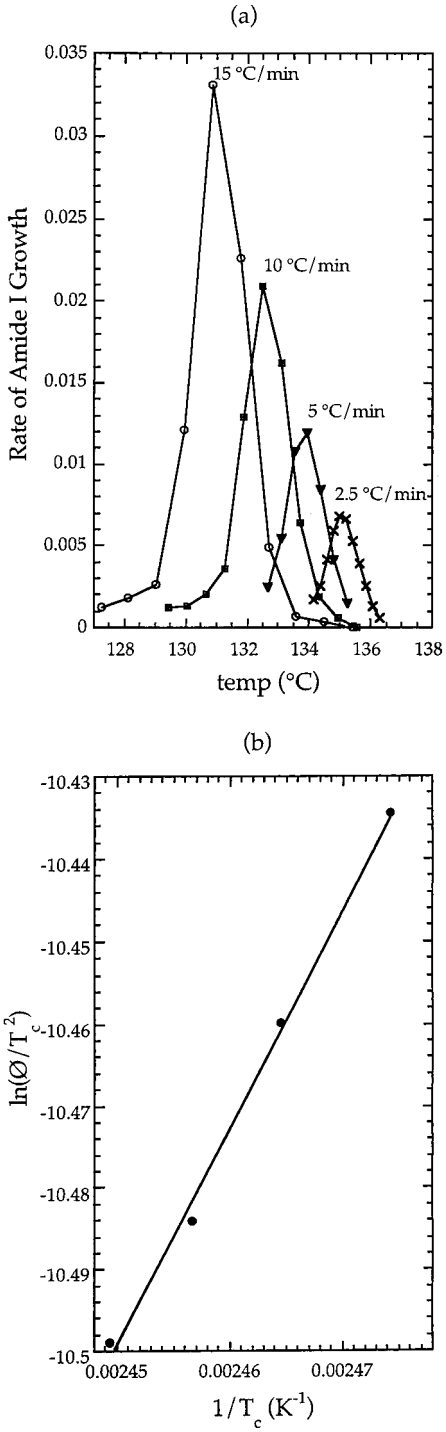


**Figure 8.** Crystallization of 22,8 PU at different cooling rates: (a) primary crystal growth rates determined from changes in the band intensity at 1685 cm$^{-1}$ with time; (b) determination of the enthalpy change ($\Delta E$) associated with primary crystallization using an Arrhenius-type approach.

higher cooling rates. Conversely, the maximum occurs with smaller supercooling, but at lower rates, for lower cooling rates. These observations are expected for the polymer crystallization process.[28] Most studies on polymer thermal crystallization have used differential scanning calorimetry (DSC) as the principal technique. The spectroscopy method shown here provides information at a much more localized level. These crystal growth rates can now be used to obtain the change in enthalpy ($\Delta E$) for the primary crystallization. For example, using the simple relation based on modification of the Arrhe-

nius equation to account for cooling rate[29−31]

$$\ln\left(\frac{\Phi}{T_c^2}\right) = -\frac{\Delta E}{RT_c} + \text{const} \qquad (5)$$

where $\Phi$ is the cooling rate (positive values) and $T_c$ is the peak crystallization temperature; $\Delta E$ for crystallization can be found by plotting $\ln(\Phi/T_c^2)$ vs $1/T_c$. As shown in Figure 8b, we found $\Delta E$ to be $-22.01$ kJ mol$^{-1}$.

Using the correlation between $\Delta\nu_{NH}$ and $\Delta H_{HB}$ described above, we can also obtain the $\Delta H_{HB}$ of the initial crystal. We find $\Delta H_{HB}$ is $-22.93$ kJ mol$^{-1}$ repeat. After accounting for the amount of ordered hydrogen bonds that are obtained by converting free urethanes (56% with $H_{free} - H_{ordered\ HB} = -22.93$ kJ mol$^{-1}$ repeat) vs disordered hydrogen bonds (44% $H_{disordered\ HB} - H_{ordered\ HB} = -8.71$ kJ mol$^{-1}$ repeat), the total contribution from hydrogen bonding is $-16.67$ kJ mol$^{-1}$ repeat. On the basis of a comparison between $\Delta E$ and the hydrogen-bonding contribution, initial crystal formation is apparently driven almost entirely by the interchain interactions between urethane units. The methylene chain seems to contribute little to the enthalpy of this initial crystal.

Nucleation is typically described as a competition between the surface vs the bulk free energy. These terms are directly related to the energy of creating a fold, the loss of translational entropy, and the stability from crystalline interactions.[3,32,33] The total free energy thus depends on the size of the nucleus. Smaller nuclei will not be stable due to the large unfavorable contribution from the surface terms. In a system of strongly interacting chains, the molten phase consists of a distribution of free and hydrogen-bonded states. Hydrogen bonds stabilize an interaction between chains with little entropic penalty. In fact, 75% of the urethane units are interacting in the molten phase of 22,8 PU. Clearly, the system is in a state where pairwise "nuclei" are already stable. In other words, the free energy change associated with nucleus size should be perturbed to favor smaller nuclei.

An energy diagram of the thermal crystallization of 22,8 PU can be postulated, as shown in Figure 9. The free energy of the melt depends on the equilibrium constant between free and hydrogen-bonded species. As the temperature is increased, the number of free urethanes will increase. A completely free state can never be observed, however, before the polymer decomposes. Thus, starting with 75% of the urethanes interacting initially, primary crystal formation shows an enthalpic gain comparable to the hydrogen bond strength and a structure where 12% of the urethanes and methylene segments exhibit order. The secondary crystallization stage shows order increases in the hydrogen bonds to 25%, but the methylene segments order to a greater extent of 40%. The enthalpy of fusion ($\Delta H_f$) obtained from DSC ($-45.60$ kJ mol$^{-1}$)[22] shows that the overall enthalpic gain during secondary crystallization is $-23.60$ kJ mol$^{-1}$.

These values suggest that for this system of polymers hydrogen bonding is the dominant term initially. In the melt, 22,8 PU is seen as a physically cross-linked network. This phase then evolves into order driven by the ordering of hydrogen bonds into an initial crystal. The perfection of this crystal is expected to be very low. Later stages of crystal growth and perfection are dominated by the flexible methylene chain. Studies have shown that both the strength and the range of interactions between protein molecules is crucial for crystal nucleation and the eventual growth. An aggregate can first form followed by a transition to the ordered phase.[34] Our spectroscopic data have characterized the initial stage of order and the various stages of order evolution for 22,8 PU.

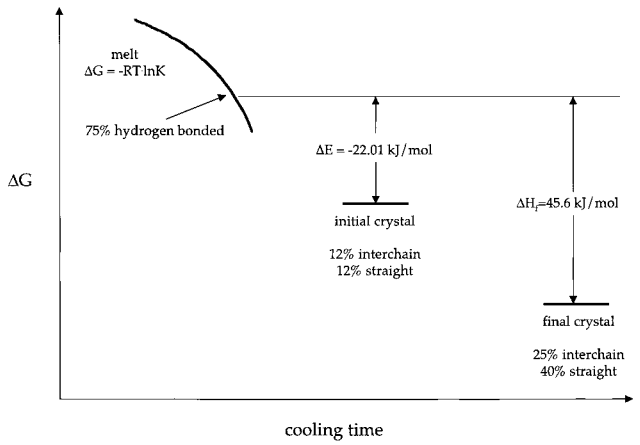


**Figure 9.** Change in free energy for 22,8 PU crystallized from melt. The cooling rate from 160 °C is maintained at 5 °C min$^{-1}$.

## Conclusions

In this spectroscopy study, we have followed the crystallization behavior of polymethylene chains with strong interacting groups placed periodically along the chain. The kinetics is characterized by three stages: (1) initial crystal formation driven by the formation of ordered interchain interactions, (2) secondary crystallization which involves converting disordered hydrogen bonds and defect aliphatic segments to crystal, and (3) further ordering of aliphatic chains.

Order formation during the induction period can be observed by infrared spectroscopy. The induction period is characterized by a continuous change in the ensemble distribution of disordered amide I states. In other words, urethane geometry or interaction strength improves before "ordering." The measured $\Delta E$ for primary crystallization of $-22.01$ kJ mol$^{-1}$ also suggests that hydrogen bonding drives the initial order formation since the magnitude is comparable to $\Delta H_{HB}$ of the crystal. Thus, while 12% of the aliphatic segments are already straightened after initial crystallization, van der Waals interactions seem to contribute very little to the overall energy of the initial crystal.

During secondary crystallization, order formation in the urethane units reaches a plateau, while the aliphatic segments continue to straighten. By monitoring the disordered hydrogen bonds, it can be seen that as the temperature is lowered, more favorable geometries are continuously formed. While thermal crystallization occurs, this composite band increases in width and the average intensity shifts to lower wavenumber. Growth in these domains is severely inhibited. The ultimate structure shows a dramatic difference between the order characterized by interchain interactions (25%) and that shown by conformational perfection (40%). In our experiment, hydrogen bonds are observed in the molten phase. Similarly, the hydrogen bonds also exist in the crystals. We would presume that hydrogen bonds exist at every phase measured. Our observations would support a picture of structural evolution.

## References and Notes


(1) Hoffman, J. D.; Miller, R. L. *Polymer* **1997**, *38*, 3151.
(2) Sadler, D. M.; Gilmer, G. H. *Phys. Rev. B* **1988**, *38*, 5684.
(3) Wunderlich, B. *Macromolecular Physics*; Academic Press: New York, 1976; Vol. 2, Chapter 6.
(4) Gandica, A.; Magill, J. H. *Polymer* **1972**, *13*, 595.
(5) Matsuba, G.; Kanaya, T.; Saito, M.; Kaji, K.; Nishida, K. *Phys. Rev. E* **2000**, *62*, R1497.
(6) Imai, M.; Mori, K.; Mizukami, T.; Kaji, K.; Kanaya, T. *Polymer* **1992**, *33*, 4457.
(7) Strobl, G. *Acta Polym.* **1997**, *48*, 562.
(8) Kohan, M. I. *Nylon Plastics Handbook*; Carl Hanser Verlag: New York, 1995.
(9) Tashiro, K.; Sasaki, S.; Kobayashi, M. *Macromolecules* **1996**, *29*, 7460.
(10) Healey, A. M.; Hendra, P. J.; West, Y. D. *Polymer* **1996**, *37*, 4009.
(11) McKiernan, R. L.; Gido, S. P.; Penelle, J. *Polymer*, in press.
(12) Coleman, M. M.; Lee, K. H.; Skrovanek, D. J.; Painter, P. C. *Macromolecules* **1986**, *19*, 2149.
(13) Snyder, R. G. *J. Chem. Phys.* **1967**, *47*, 1316.
(14) Skrovanek, D. J.; Painter, P. C.; Coleman, M. M. *Macromolecules* **1986**, *19*, 699.
(15) Tsubomura, H. *J. Chem. Phys.* **1956**, *24*, 927.
(16) Stolov, A. A.; Borisover, M. D.; Solomonov, B. N. *J. Phys. Org. Chem.* **1996**, *9*, 241.
(17) Coleman, M. M.; Graf, J. F.; Painter, P. C. *Specific Interactions and the Miscibility of Polymer Blends*; Technomic Publishing Co.: Lancaster, 1991.
(18) Jasse, B.; Tassin, J. F.; Monnerie, L. *Prog. Colloid Polym. Sci.* **1993**, *92*, 8.
(19) Maklakov, L. I.; Furer, V. L.; Alekseev, V. V.; Furer, A. L. *Zh. Prikl. Spektrosk.* **1979**, *31*, 691.
(20) Snyder, R. G.; Schachtschneider, J. H. *Spectrochim. Acta* **1963**, *19*, 85.
(21) Wendoloski, J. J.; Gardner, K. H.; Hirschinger, J.; Miura, H.; English, A. D. *Science* **1990**, *247*, 431.
(22) McKiernan, R. L.; Heintz, A. M.; Hsu, S. L.; Gido, S. P.; Penelle, J. *Polym. Mater. Sci. Eng.* **2001**, *84*, 416.
(23) Barnes, J. D.; Fanconi, B. M. *J. Chem. Phys.* **1972**, *56*, 5190.
(24) Matsuba, G.; Kaji, K.; Nishida, K.; Kanaya, T.; Imai, M. *Macromolecules* **1999**, *32*, 8932.
(25) Imai, M.; Kaji, K.; Kanaya, T. *Phys. Rev. Lett.* **1993**, *71*, 4162.
(26) Ezquerra, T. A.; Lopez-Cabarcos, E.; Hsiao, B. S.; Balta-Calleja, F. J. *Phys. Rev. E* **1996**, *54*, 989.
(27) Ryan, A. J.; Fairclough, J. P. A.; Terrill, N. J.; Olmstead, P. D.; Poon, W. C. K. *Faraday Discuss.* **1999**, 13.
(28) Liu, S. Y.; Yu, Y. N.; Cui, Y.; Zhang, H. F.; Mo, Z. S. *J. Appl. Polym. Sci.* **1998**, *70*, 2371.
(29) Kissinger, H. E. *J. Res. Natl. Bur. Stand.* **1956**, *57*, 217.
(30) Li, Y. J.; Zhu, X. Y.; Yan, D. Y. *Polym. Eng. Sci.* **2000**, *40*, 1989.
(31) Di Lorenzo, M. L.; Silvestre, C. *Prog. Polym. Sci.* **1999**, *24*, 917.
(32) Keller, A. *Rep. Prog. Phys.* **1968**, *31*, 623.
(33) Wunderlich, B. *Macromolecular Physics*; Academic Press: New York, 1973; Vol. 2, Chapter 5.
(34) ten Wolde, P. R.; Frenkel, D. *Science* **1997**, *277*, 1975.


MA011794K